5th International Conference on Biaxial/Multiaxial Fatigue and Fracture
Cracow'97, Poland

Takamoto ITOH*, Takumi NAKATA*, Masao SAKANE**
Masateru OHNAMI**

Nonproportional Low Cycle Fatigue of 6061 Aluminum Alloy Under 14 Strain Paths

*Department of Mechanical Engineering, Faculty of Engineering, Fukui University, Japan
**Faculty of Science and Engineering, Ritsumeikan University, Japan

Keywords : Low cycle fatigue, Multiaxial stress, Nonproportional loading, Life prediction, 6061 aluminum alloy.

ABSTRACT : This paper studies the nonproportional low cycle fatigue of 6061 aluminum alloy under 14 strain paths. Tension-torsion low cycle fatigue tests were carried out using hollow cylinder tube specimens (OD 12 mm, ID 9 mm, gage length 6.4 mm) under 14 proportional and nonproportional cyclic strain paths at room temperature. Nonproportional strain written with only strain path and having a material constant correlated nonproportional fatigue lives within a factor of two scatter band. The additional hardening of 6060 aluminum alloy under nonproportional straining was also discussed in relation with fatigue life.

Notation

$\varepsilon_1(t)$ Maximum principal strain at time t
$\varepsilon_3(t)$ Minimum principal strain at time t
$\varepsilon_I(t)$ Maximum absolute value of the principal strain at time t : Max $[|\varepsilon_1(t)|, |\varepsilon_3(t)|]$
$\varepsilon_{I\,max}$ Maximum value of $\varepsilon_I(t)$ in a cycle
$\varepsilon^*(t)$ Equivalent strain based on COD at time t
$\phi(t)$ Principal strain ratio at time t
$\Delta\varepsilon_I$ Maximum principal strain range under nonproportional straining
$\Delta\varepsilon_{ASME}$ Equivalent strain range defined in Code Case N-47
$\Delta\varepsilon^*_I$ Equivalent strain range based on COD under nonproportional straining
$\Delta\varepsilon_{NP}$ Nonproportional strain range
$\Delta\varepsilon^*_{NP}$ Nonproportional strain range based on COD
$\sigma_1(t)$ Maximum principal stress at time t
$\sigma_3(t)$ Minimum principal stress at time t
$\sigma_I(t)$ Maximum absolute value of the principal stress at time t : Max $[|\sigma_1(t)|, |\sigma_3(t)|]$
$\Delta\sigma_I$ Maximum principal stress range under nonproportional straining

$\xi(t)$ Angle between the principal strain directions of $\varepsilon_I(t)$ and $\varepsilon_{I\,max}$

f_{NP} Nonproportional factor

f^*_{NP} Nonproportional factor based on COD

α Material constant which expresses the amount of additional hardening

N_f Number of cycles to failure

Introduction

ASME Code Case N-47 (1) has been frequently used as a design criterion for nonproportional low cycle fatigue, but recent studies have shown that the Code Case estimates unconservative lives for nonproportional fatigue. Nonproportional loading reduces the low cycle fatigue life due to the additional hardening depending on strain history, so the nonproportional parameter must take account of the additional hardening. A couple of nonproportional parameters which include the stress range or amplitude have been proposed (2-4), and stress terms in the parameters are able to be calculated using the inelastic constitutive equation (5-8), but it is not a simple procedure in general and requires many material constants. There is no well established method of estimating nonproportional low cycle fatigue lives based on only strain history.

The authors (9) carried out nonproportional low cycle fatigue tests using a hollow cylinder specimen of Type 304 stainless steel and proposed a nonproportional low cycle parameter written with only strain history. Type 304 stainless steel is known as a material which shows the large additional hardening under nonproportional loadings (5, 9-11). Fatigue lives drastically reduce by additional hardening which depends on strain history. The maximum reduction is a factor of 10 when compared with the proportional fatigue life. However, the degree of additional hardening is material dependent, so that the reduction of nonproportional lives is also material dependent.

The aim of this paper is to examine the nonproportional low cycle fatigue life of 6061 aluminum alloy which shows a small additional hardening and to confirm the availability of the nonproportional strain proposed previously to the small additional hardening material, by making extensive nonproportional low cycle fatigue tests using 14 strain paths.

Experimental Procedure

The material tested was 6061 aluminum alloy (6061 Al alloy) which received T6 heat treatment. Mises' equivalent total strain controlled nonproportional low cycle fatigue tests were carried out using hollow cylinder specimens with 9 mm inner diameter, 12 mm outer diameter and 6.4 mm gage length as shown in Fig.1. Test machine used was a tension-compression and reversed torsion electric servo hydraulic low cycle fatigue machine.

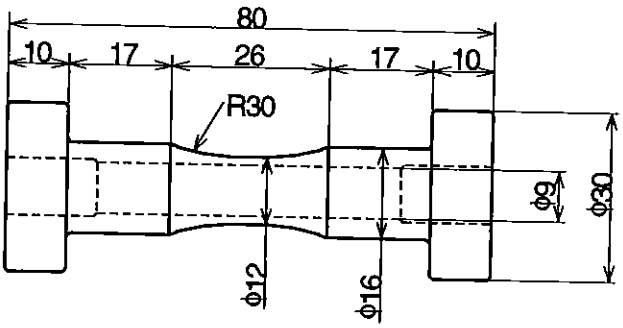

Fig.1 Shape and dimensions of the specimen tested (mm).

Figure 2 shows strain paths employed, where ε and γ are the axial and shear strains, respectively. Case 0 is a push-pull test and is the base data used for the nonproportional life prediction. Total axial strain range was varied from 0.5 % to 1.5 %. Strain paths shown in the figure were determined so as to make clear the various effects in nonproportional straining (9). In strain paths 1-13, the total axial strain range, $\Delta\varepsilon$, had the same strain magnitude as the total shear strain range, $\Delta\gamma$, on Mises' equivalent basis.

In this paper, one cycles is defined as full straining for both axial and shear cycles. Thus, a complete straining along the strain paths shown in Fig.2 was counted as one cycle for all the Cases except Case 3 and 4. In Case 3 and 4, a complete cycling was counted as two cycles. The number of cycles to failure (N_f) was defined as the cycle at which the axial stress amplitude was decreased by 5 % from its cyclically stable value.

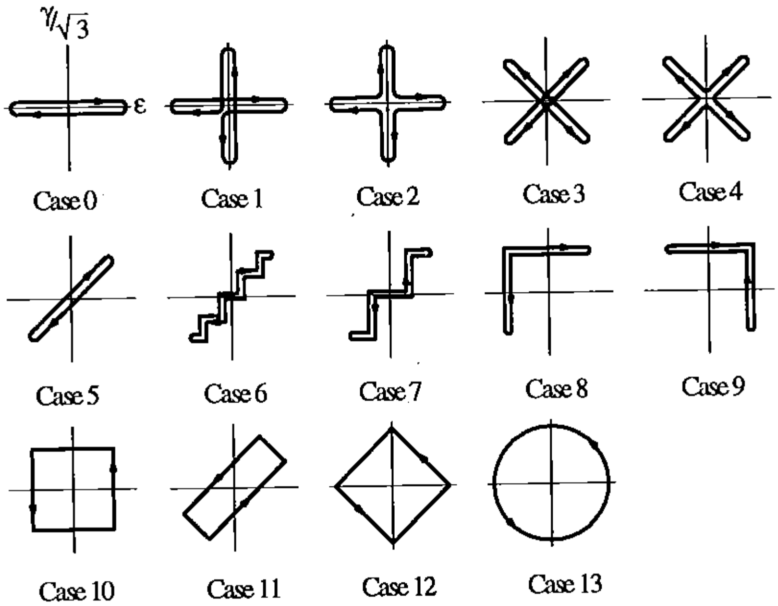

Fig.2 Proportional and nonproportional strain paths.

Experimental Results and Discussion

Definition of Stain and Stress Ranges This study defined the maximum principal strain range as

$$\Delta\varepsilon_I = \mathrm{Max}\left[\varepsilon_{I\max} - \cos\xi(t)\cdot\varepsilon_I(t)\right] \quad (1)$$

where $\varepsilon_I(t)$ is the maximum absolute value of principal strain at time t and is given by Eq.2.

$$\varepsilon_I(t) = \begin{cases} |\varepsilon_1(t)| & \text{for } |\varepsilon_1(t)| \geq |\varepsilon_3(t)| \\ |\varepsilon_3(t)| & \text{for } |\varepsilon_1(t)| < |\varepsilon_3(t)| \end{cases} \quad (2)$$

where $\varepsilon_1(t)$ and $\varepsilon_3(t)$ are the maximum and minimum principal strains at time t, respectively. The maximum value $\varepsilon_{I\max}$ of $\varepsilon_I(t)$ is expressed as

$$\varepsilon_{I\,max} = \mathrm{Max}\left[\varepsilon_I(t)\right] \tag{3}$$

$\xi(t)$ is the angle between $\varepsilon_{I\,max}$ and $\varepsilon_I(t)$ directions and expresses the variation angle of the principal strain direction.

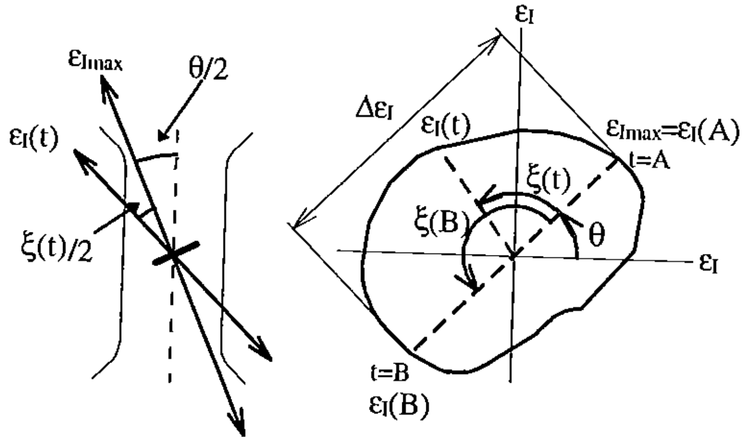

Fig.3 Schematic graph of $\varepsilon_I(t)$, $\xi(t)$ and $\Delta\varepsilon_I$.

Figure 3 schematically shows the relationship between $\varepsilon_I(t)$ and $\xi(t)$ on a polar figure of $\varepsilon_I(t)$. The angle $\xi(t)$ becomes a half value in physical plane i.e., in the specimen. The principal strain range, $\Delta\varepsilon_I$, is determined by two strains, $\varepsilon_I(A)$ and $\varepsilon_I(B)$, and the angle between them, where A and B are the times maximizing the strain range in bracket in Eqs.1 and 3. Thus, equation (1) is equivalent to finding the largest principal strain range occurred in specimen and is rewritten as,

$$\begin{aligned} \Delta\varepsilon_I &= \varepsilon_I(A) - \cos\xi(B)\cdot\varepsilon_I(B) \\ \varepsilon_I(A) &= \varepsilon_{I\,max} \end{aligned} \tag{4}$$

The angle $\xi(B)$ is the angle between the principal strain directions of ε_{Imax} and $\varepsilon(B)$.

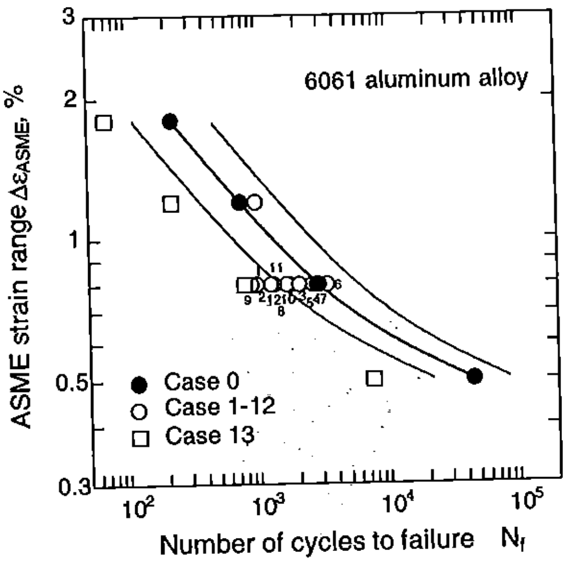

Fig.4 Correlation of nonproportional LCF lives of 6061 aluminum alloy with ASME strain range.

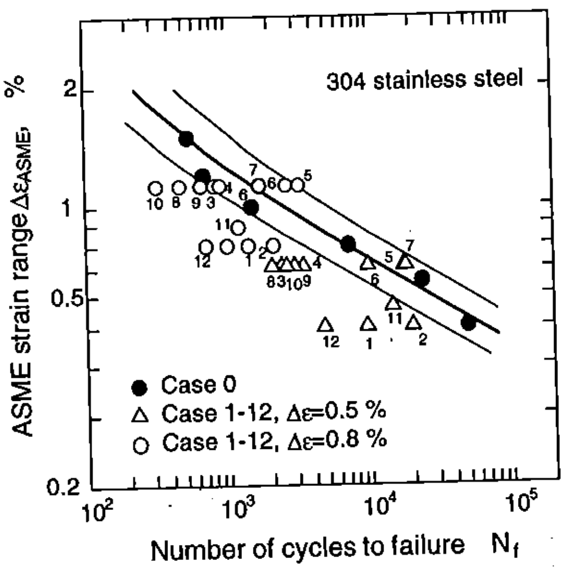

Fig.5 Correlation of nonproportional LCF lives of Type 304 stainless steel with ASME strain range.

Nonproportional Low Cycle Fatigue Life

Figure 4 shows the correlation of nonproportional low cycle fatigue (LCF) lives of 6061 Al alloy with the equivalent strain range defined in ASME Code Case N-47 (ASME strain range) (1), which has been used as a design parameter for the nonproportional fatigue. In the figure, a factor of two scatter band is shown by lines based on the push-pull data, i.e., Case 0 data, and attached numbers denote the Case number. ASME strain range correlates fatigue lives unconservatively for some Cases by more than a factor of two. The lowest fatigue lives occurred in Case 13, i.e., circular path. Fatigue lives in that Case are about 1/3 of those in Case 0. The significant reduction in fatigue life also occurred in Case 10 and 12, box paths, as well as circular path.

For the comparison, the data correlation of Type 304 stainless steel with ASME strain is shown in Fig.5, of which tests were made by the authors (9). Specimen shape and strain paths are same as those in this study. The figure shows the same trend of the data correlation as that in Fig.4, but ASME strain gives a more unconservative estimate for Type 304 steel than 6061 Al alloy. The minimum lives are found in Case 12 which is about 10 % of the failure cycle in Case 0 at the same strain range, whereas it is about 30% for 6061 Al alloy.

Comparison of the results between Fig.4 and Fig.5 leads to the conclusion that the nonproportional LCF damage is a function of strain history and material. Thus, nonproportional strain parameter must take account of these two factors.

Stress Under Nonproportional Straining

Figures 6 (a) and (b) show the correlation of LCF lives of 6061 Al alloy and Type 304 steel with maximum principal stress range, $\Delta\sigma_I$, defined by Eq.5 similar to that of $\Delta\varepsilon_I$,

$$\Delta\sigma_I = \sigma_I(A) - \cos\xi(B)\cdot\sigma_I(B) \qquad (5)$$

$$\sigma_I(t) = \begin{cases} |\sigma_1(t)| & \text{for} \quad |\sigma_1(t)| \geq |\sigma_3(t)| \\ |\sigma_3(t)| & \text{for} \quad |\sigma_1(t)| < |\sigma_3(t)| \end{cases}$$

where $\sigma_1(t)$ and $\sigma_3(t)$ are the maximum and minimum principal stresses at time t. Fatigue lives of 6061 Al alloy, Fig.6 (a), are mostly within a factor of two band, while those of Type

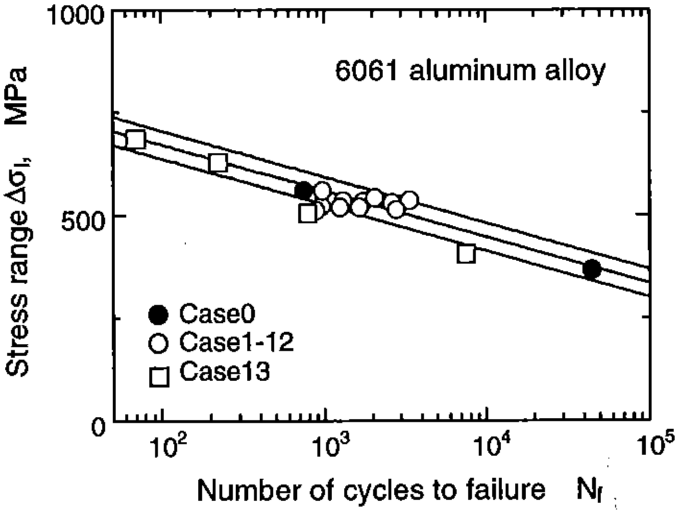

(a) 6061 aluminum alloy

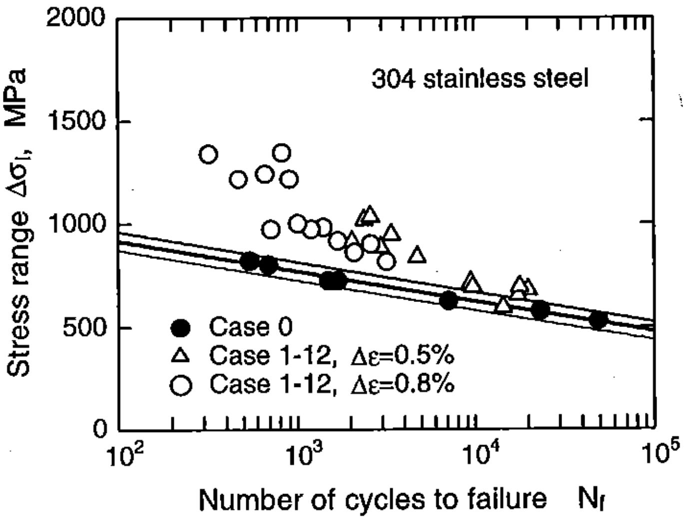

(b) Type 304 stainless steel

Fig.6 Correlation of nonproportional LCF liveswith principal stress range.

304 steel, Fig.6 (b), are correlated too conservatively where most of the data are out of a factor of two scatter band. The results in these two figures indicate that the small reduction in LCF life occurs for small additional hardening material and the large reduction for large additional hardening material. The maximum principal stress range is a suitable parameter for the former material but is not for the latter material.

Reduction in nonproportional LCF life is connected with the degree of additional hardening (2-4). In nonproportional loading, the principal strain direction is changed with proceeding cycles, so the maximum shear stress plane is changed continuously in a cycle. This causes an interaction between slip systems and which results in the formation of small cells (10,11) for Type 304 steel. Large additional hardening occurred by the interaction of slip systems for that steel. 6061 Al alloy, on the other hand, is a material of high stacking fault energy and slips of dislocations are wavy. No large interaction occurred in 6061 Al alloy since dislocations change their glide planes easily following the variation of the maximum principal strain direction (11).

Nonproportional LCF Strain Parameter

The authors proposed nonproportional strain range, $\Delta\varepsilon_{NP}$, below.

$$\Delta\varepsilon_{NP} = \left(1+\alpha \cdot f_{NP}\right) \cdot \Delta\varepsilon_I \tag{6}$$

where α is a material constant related to the additional hardening. f_{NP} is the nonproportional factor which expresses the severity of nonproportional straining and is described by only the strain history.

The results in Fig.6 showed that the degree of additional hardening is material dependent. Other literature reported that aluminum alloys show little or no additional hardening (3,4,10), while Type 304 stainless steel usually gives a significant additional hardening (5,10,11). Doong et al. (10) have reported that little additional hardening has almost no effect on nonproportional fatigue life and significant additional hardening causes a drastic reduction in fatigue life. Thus, the nonproportional LCF parameter must include a parameter which expresses the amount of additional hardening.

Equation 6 takes account of the amount of additional hardening by the material constant, α. The value of α is defined as the ratio of stress amplitude under 90 degrees out-of-phase loading (circular strain path in $\gamma/\sqrt{3}$-ε plot) to that under proportional loading. 90 degrees out-of-phase loading shows the maximum additional hardening among all the nonproportional histories (3,12). For 6061 Al alloy, the stress amplitude under 90 degrees out-of-phase loading was increased up to 20% in comparison with the proportional loading, so the value of α is 0.2. For Type 304 stainless steel, it was 0.9 due to the large additional hardening (3,9).

The nonproportional factor which expresses the severity of nonproportional straining is defined as

$$f_{NP} = \frac{k}{T\cdot\varepsilon_{I\,max}} \int_0^T \left(\left| \sin\xi(t) \right| \cdot \varepsilon_I(t) \right) dt \qquad (7)$$

$$k = \frac{\pi}{2}$$

where $\varepsilon_I(t)$, $\varepsilon_{I\,max}$ and $\xi(t)$ are the parameters defined in Eqs.1-3 and Fig.3. T is time for a cycle and f_{NP} is normalized by T and $\varepsilon_{I\,max}$. k is a constant to make f_{NP} unity under 90 degrees out-of-phase loading. The reason for making f_{NP} integral form is that the experimental results indicate that the nonproportional LCF life is significantly influenced by the degree of principal strain direction change and strain length after the direction change. The value of f_{NP} takes zero for proportional straining. In Eq.7, f_{NP} is calculated from only the strain path and accounts for the severity of nonproportional loading. The parameter given by Eq.6 in this study would evaluate the degree of additional hardening due to nonproportional loading.

The authors (13) proposed another nonproportional strain on the basis of the equivalent strain based on crack opening displacement (COD strain) to improve the data correlation of proportional LCF lives. The COD strain physically expresses the intensity of COD in multiaxial stress and strain states. The nonproportional strain range based on COD is defined similar to Eq.6 as,

$$\Delta\varepsilon^*_{NP} = (1+\alpha f^*_{NP})\,\Delta\varepsilon^*_I \qquad (8)$$

where $\Delta\varepsilon^*_I$ is the COD strain range under nonproportional straining and is given by

$$\Delta\varepsilon^*_I = \varepsilon^*(A) - \cos\xi(B)\cdot\varepsilon^*(B) \qquad (9)$$

$$\varepsilon^*(t) = \beta\cdot(2-\phi(t))^{m'}\cdot\varepsilon_I(t)$$

In this equation, $\varepsilon^*(t)$ and $\phi(t)$ are the COD strain and the principal strain ratio at time t. $\phi(t)$ is defined as

$$\phi(t)=\begin{cases} \varepsilon_3(t)/\varepsilon_1(t) & \text{for} \quad |\varepsilon_1(t)| \geq |\varepsilon_3(t)| \\ \varepsilon_1(t)/\varepsilon_3(t) & \text{for} \quad |\varepsilon_1(t)| < |\varepsilon_3(t)| \end{cases} \tag{10}$$

Constants, β and m', in Eq.9 take the values of 1.83 and -0.66, respectively, independent of material which was verified by FEM analyses (13). The nonproportional factor based on COD strain, f^*_{NP}, is given by

$$f^*_{NP}=\frac{k^*}{T\cdot\varepsilon^*_{I\max}}\int_0^T\left(\left|\sin\xi(t)\right|\cdot\varepsilon^*(t)\right)dt \qquad k^*=1.66 \tag{11}$$

Figures 7 and 8 correlate the nonproportional fatigue data with the two nonproportional strains shown in Eqs.6 and 8, respectively. In these figures, (a) and (b) are the correlation of fatigue lives for 6061 Al alloy and Type 304 steel, respectively. Almost all the nonproportional data are within a factor of two scatter band in the correlation with the two nonproportional strains. The scatter of the data appears to be somewhat smaller in the correlation with $\Delta\varepsilon^*_{NP}$, which arises from the better correlation of proportional data with COD strain range than that with the maximum principal strain range (13). Therefore, the two nonproportional strains proposed by Eqs.6 and 8 are able to predict nonproportional LCF lives with various strain histories. These equations have only one material constant which is determined by the stress range ratio under 90 degrees out-of-phase and proportional loadings.

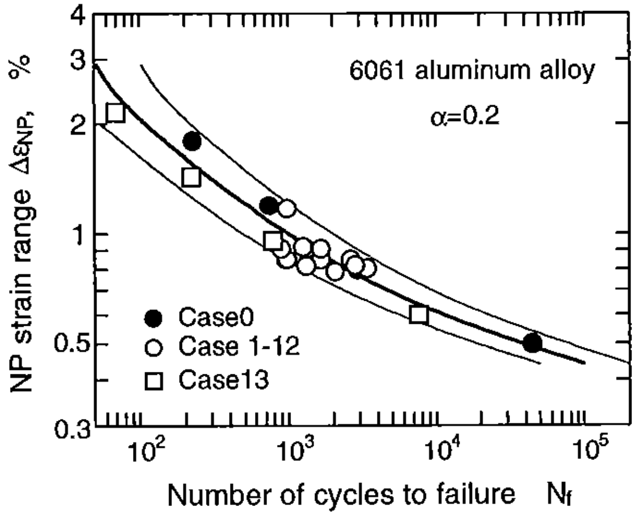

(a) 6061 aluminum alloy

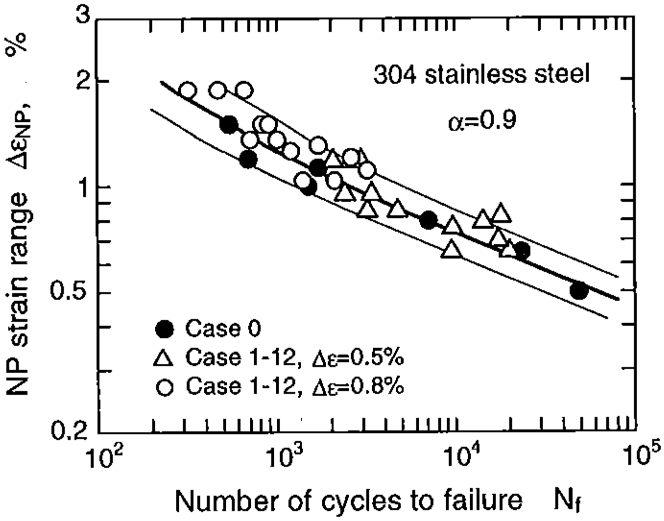

(b) Type 304 stainless steel

Fig.7 Correlation of nonproportional LCF lives with the nonproportional LCF strain range based on the principal strain.

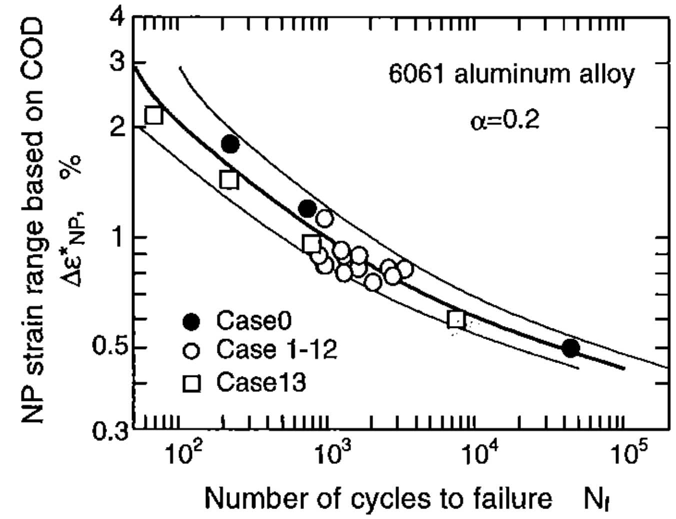

(a) 6061 aluminum alloy

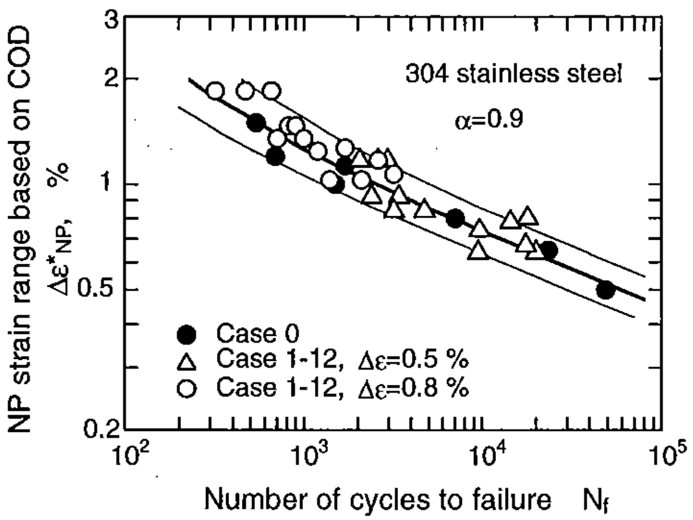

(b) Type 304 stainless steel

Fig.8 Correlation of nonproportional LCF lives with the nonproportional LCF strain range based on COD.

Conclusion

Proportional and nonproportional low cycle fatigue tests were carried out using fourteen strain paths for 6061 aluminum alloy hollow cylinder specimens at room temperature. Fatigue lives of 6061 aluminum alloy were reduced by nonproportional loading but the reduction was not so large as that of Type 304 stainless steel. The two nonproportional strains were applied nonproportional LCF lives of the two material. The scatter of the data was within a factor of two for both the materials and which indicates the two strains are suitable parameter for correlating nonproportional LCF data of small and large additional hardening materials.

References

(1) ASME Code Case N-47, (1978), Case of ASME Boiler and Pressure Vessel Code, Case N-47, Class 1, Section 3, Division 1, ASME.

(2) Smith R. N., Watson P. and Topper T. H., (1970), A Stress Strain Function for the Fatigue of Materials, J. Materials JMLSA, Vol.5, No.4, pp.767-778.

(3) Socie D. F., (1987), Multiaxial Fatigue Damage Models, Trans. ASME J. Engng. Mater. Technol., Vol.109, No.4, pp.293-298.

(4) Fatemi A. and Socie D. F., (1988), A Critical Plane Approach to Multiaxial Fatigue Damage Including Out-of-Phase Loading, Fatigue and Fracture of Engng. Mater. and Struct., Vol.11, No.3, pp.149-165.

(5) McDowell D. L., (1983), On the Path Dependence of Transient Hardening and Softening to Stable States Under Complex Biaxial Cyclic Loading. Proc. Int. Conf. on Constitutive Laws for Engng. Mater., Tucson, AZ, (Desai and Gallagher, eds.), p.125.

(6) Krempl E. and Lu H., (1983), Comparison of the Stress Responses of an Aluminum Alloy Tube to Proportional and Alternate Axial and Shear Strain Paths at Room Temperature, Mechanics of Materials, Vol.2, pp.183-192.

(7) Benallal A. and Marquis D., (1987), Constitutive Equations for Nonproportional Cyclic Elasto -Viscoplasticity, Trans. ASME J. Engng. Mater. Technol., Vol.109, No.4, pp.326-336.

(8) Doong S. H. and Socie D. F., (1991), Constitutive Modeling of Metals Under Nonproportional Loading, Trans. ASME J. Engng. Mater. Technol., Vol.113, No.1, pp.23-30.

(9) Itoh T, Sakane M, Ohnami M. and Socie D. F., (1995), Nonproportional Low Cycle Fatigue Criterion for Type 304 stainless Steel, Trans. ASME J. Engng. Mater. Technol., Vol.117, No.3, pp.285-292.

(10) Doong S. H., Socie D. F. and Robertson, (1990), I. M. Dislocation Substructures and Nonproportional Hardening, Trans. ASME J. Engng. Mater. Technol., Vol.112, No.4, pp.456-465.

(11) Itoh T., Sakane M., Ohnami M. and Ameyama K., (1992), Additional Hardening due to Nonproportional Loading (A Contribution of Stacking Fault Energy), MECAMAT'92, Proc. Int. Seminar on Multiaxial Plasticity, France, (Benallal et al. eds.), pp.43-50.

(12) Kanazawa K., Miller K. J. and Brown M. W., (1979), Cyclic Deformation of 1%Cr-Mo-V Steel Under Out-of-Phase Loads, Fatigue Engineering Materials and Structures, Vol.2, No.2, pp.217-228.

(13) Itoh T., Sakane M. and Ohnami M., (1994), High Temperature Multiaxial Low Cycle Fatigue of Cruciform Specimen, Trans. ASME J. Engng. Mater. Technol., Vol.116, No.1, pp.90-98.